Ninth International Conference on Advances in Steel Structures (ICASS'2018)
5-7 December 2018 - Hong Kong, China

THE EFFECTS OF AXIAL TENSION ON THE SAGGING-MOMENT REGIONS OF CONCRETE-FILLED TUBULAR FLANGE GIRDERS

R. Al-Dujele [1]*and K.A. Cashell [1]

[1] Brunel University London, London, UK
E-mails: rana.al-dujele@brunel.ac.uk, katherine.cashell@brunel.ac.uk

Abstract: *Steel-concrete composite construction is commonly used for many types of structure, including heavy load-bearing applications such as bridges and multi-storey car parks. Some of their component elements such as bridge approaches, inclined parking ramps and stadium beams are exposed to a simultaneous combination of high axial loads and bending moments. A relatively new solution for heavily loaded composite members are concrete-filled tubular flange girders (CFTFGs) which are unconventional I-shaped girders where one or both of the steel flanges are replaced with a hollow section and then filled with concrete to increase the strength and stiffness. These are complex members and their behaviour is governed by a number of inter-related parameters. This work aims to investigate the ultimate strength of CFTFGs with a stiffened web under the combined effects of various levels of axial tension and positive (sagging) bending moment. Nonlinear three-dimensional finite element (FE) analyses using the ABAQUS computer software package are employed to conduct parametric studies. Several influential parameters are examined and conclusions are discussed.*

Keywords: Concrete-filled tubular flange girders; Axial tension; Sagging moment; Finite element analysis; Combined loading; Interaction diagram.

DOI: 10.18057/ICASS2018.P.009

1 INTRODUCTION

Steel-concrete composite structural designs have been used in a wide variety of applications in recent decades because of their advantages relative to other construction methods. The optimum use of the two constituent materials given their respective advantages, such as steel strength and ductility in the tension zone and concrete robustness and high stiffness in the compression zone, results in a very efficient structural solution. Beams can often be exposed to combined actions, in continuous or semi-continuous structures, where members are under either positive (sagging) or negative (hogging) bending moments. The most efficient use of the materials' strengths occurs when the beam is exposed to positive bending at the mid-span. In this study, the steel component is subjected to tensile forces and the concrete component is mainly in compression, therefore harnessing the best attributes of each material [1].

Concrete filled tubular flange girders (CFTFGs) are unconventional composite beams comprising an I-shaped steel section which has the flat top flange replaced with a hollow structural member which is filled with concrete. The resulting section offers very high lateral torsional buckling strength and stiffness compared with conventional steel I-beams of similar depth, width and weight, typically leading to a reduction in lateral bracing requirements for CFTFGs [2]. Hence, several researchers have investigated using concrete filled tubular flange girders in heavy loading scenarios, such as bridge applications, car parks and multi-storey

buildings. It has been shown that torsional deformations can be reduced or even prevented by substituting the conventional flat plated top flange with a hollow tubular flange [3,4]. This is because the hollow flange improves the twisting resistance of the beam compared with open sections and decreases their sensitivity to lateral-torsional buckling. It is noteworthy though that since the hollow section flange has high torsional stiffness, the web of the girder is comparatively flexible, and therefore the flexural strength of the section can be reduced by web distortion.

Early studies at Lehigh University in the USA tested two 18 m long CFTFGs with a rectangular concrete filled tube as the compression flange and a flat plate as the tension flange, as depicted in Figure 1(a) [5,6]. The results of these tests indicated that it is possible to use large un-braced lengths owing to the large torsional stiffness of the tubular flange. Kim and Sause [7] studied the performance of CFTFGs with a circular concrete filled tube as the compression flange rather than a rectangular shape, as illustrated in Figure 1(b). Some of the potential benefits of CFTFGs were summarized, including the provision of more strength, stiffness, and stability compared with a flat plate flange which uses a similar amount of steel, and also design formulas for predicting the lateral-torsional buckling (LTB) strength of CFTFGs were proposed. Generally, for the many different configurations which have been studied, it has been shown that CFTFGs bring numerous advantages compared with conventional steel girders, particularly for large spanning or heavily loaded applications, including the ability to minimize the required under-clearance, simplify erection and eliminate the need for stiffeners, cross frames or diaphragms.

Typically, for CFTFGs, the hollow structural section flange is filled with unreinforced concrete after girder fabrication in the factory, and the concrete strengthens the compression flange of the girder. The torsional stiffness and strength of the girder is considerably increased by the tube, thereby improving the lateral-torsional buckling resistance of the girder. The concrete filled tube also has the influence of reducing the depth of the web in compression, thus lowering the girder's web slenderness. This increased stability and strength of a CFTFG reduces the need for lateral bracing, compared to that of conventional plate girders, and allows for greater spans to be achieved for a similar overall depth. The increase in torsional stiffness and strength also eliminates the need for fabricating exterior girders with intermediate constructability stiffeners, as are needed in ordinary plate girders to resist overhang forces. A few transverse stiffeners along the girder length are necessary to control cross-section distortion, thus allowing the girder to achieve its lateral torsional buckling strength [2].

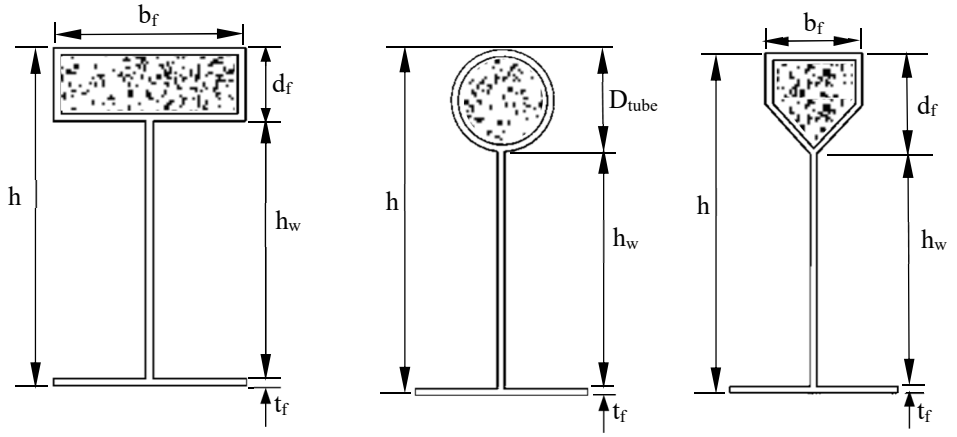

Figure 1: Girders with concrete filled tubular flanges including (a) rectangular flange, (b) circular flange and (c) pentagonal flange.

Uy and Tuem [8] were the earliest to address the effect of tension and provide a full moment–axial load interaction diagram for composite beams. The effects that the simultaneous action of axial load and bending moment have on the ultimate capacity of a CFTFG are not yet covered in a comprehensive way in the international design codes. In fact, modern steel and composite construction codes, including Eurocode 4 [9], Australian code AS2327 [10] and the American AISC [11], give detailed guidance on the design of composite columns under combined actions, but they do not address the effects of combined loading in CFTFGs, which are inherently asymmetric in nature.

This paper presents a numerical study on the behaviour of CFTFGs under the combined effects of positive bending and axial tension. Different combinations of tension and bending moment are studied, and the ultimate capacities and failure modes are identified and discussed. A finite element model has been developed in order to investigate the combined effects. The model is capable of capturing both the geometric and material nonlinearities of the behavior and available experimental data are used to validate the model. The three-dimensional model is shown to be capable of simulating the inelastic behaviour of concrete filled tubular flange girders (CFTFGs) with efficiency and to trace the failure modes up to the ultimate deformation levels. Thereafter, the FE model is employed to conduct parametric studies, in order to identify the most salient parameters on the overall performance. It is found that the moment capacity of a CFTFG section is reduced under the presence of an axial tensile force acting in the steel beam section. The tensile capacity of the CFTFGs, however, is limited by the axial capacity of the steel beam alone.

2 FINITE ELEMENT (FE) SIMULATION MODEL AND VALIDATION

2.1 FE model description

The specimen details incorporated in the FE model are based on the circular tubular flange girder which was examined in the test programme of Wang et al. [12]. Accordingly, the cross-section is 0.5 m in height and 4.3 m in length, as shown in Figure 2. Table 1 presents the principal dimensions of the tests, namely D_{tube}, t_t, h_w, t_w, b_f, t_f, and $t_{stiffener}$ which represent the tube outside diameter, tube thickness, web depth, web thickness, width of the bottom flange, thickness of the bottom flange and stiffener thickness, respectively. The beam is subjected to two concentrated loads in the vertical direction and the distance between the loading points is 1 m. There are four stiffeners along the beam length and each is 12 mm in thickness. These are located at the supports and loading points to prevent local instability of the web at these postions. Simply supported boundary conditions are employed in the FE model, replicating the experimental arrangement. The steel section is made from Q235 steel, and the material properties incorporated in the model are presented in Table 2 including the yield strength (f_y), ultimate strength (f_u), Youngs modulus (E) and Poissons ratio [13]. Also included in the table are the compressive strength (f_c) and Poissons ratio of the concrete.

Table 1: Dimensions of the CFTFG cross-section.

D_{tube} (mm)	t_t (mm)	h_w (mm)	t_w (mm)	b_f (mm)	t_f (mm)	$t_{stiffener}$ (mm)
219	8	267	6	150	14	12

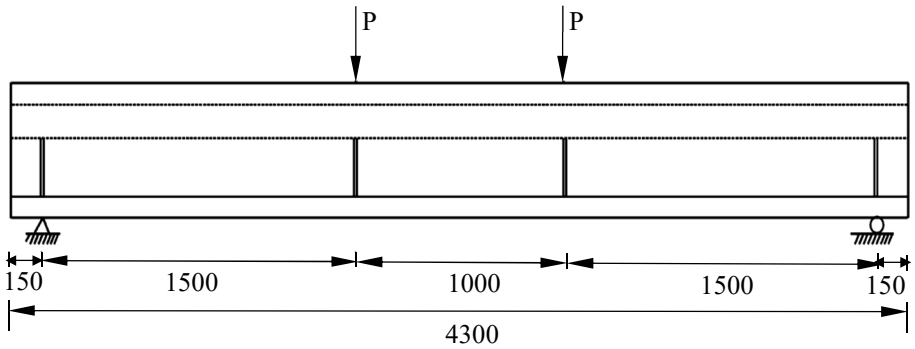

Figure 2: Schematic of the simply supported beam (all units in mm)

Table 2: Details of the material properties.

Material	Properties	Symbol	Unit	Value
Steel [13]	Yield stress	f_y	N/mm^2	287.9
	Ultimate stress	f_u	N/mm^2	430.2
	Young's modulus	E_s	N/mm^2	195000
	Poisson's ratio			0.28
Concrete	Compressive cylinder strength of concrete	f_c	MPa	38.6
	Poisson's ratio			0.20

2.2 Material modelling

In the finite element model, the concrete infill is represented using 8-noded brick elements with reduced integration, known as C3D8R in the ABAQUS library. The concrete damaged plasticity (CDP) model is employed for modelling the constitutive behaviour of the concrete. The model assumes that the infilled concrete fails either in compression, through crushing, or tension, through cracking. On the other hand, the top tubular flange, web, bottom flange and stiffeners are modelled using a four-node, three-dimensional shell element (S4R in the ABAQUS library) with reduced integration. The S4R shell element has six active degrees of freedom per node, including three displacements and three rotations. The reduced integration enables more efficient computation without compromising the accuracy of the results. A tie contact is defined between the surface of the steel section and the edges of the stiffeners. Following a mesh sensitivity study, it has been found that an element size of 30×30 mm provides the best combination of accuracy and computational efficiency and therefore is applied to all elements in the model.

2.3 Support and loading conditions

The geometry and loading conditions of the beam are symmetrical about the mid-span and therefore only half the girder length is modelled. Accordingly, one end section of the beam model has simply supported boundary conditions whilst the other end has symmetrical boundary conditions, as shown in Figure 3, in which u_x, u_y, u_z, θ_x, θ_y, and θ_z are the displacements and the rotations about the global x, y and z axes, respectively. The y-z plane is considered to be in-plane whilst the x-z and x-y planes are out-of-plane, in the current study. At the end of the beam (i.e. at the support), the vertical displacement (u_y) and lateral displacements (u_x) of all nodes along the y-axis (i.e., when x = 0), and the twist rotations about z and y-axes (θ_z and θ_y) are restrained against movement and therefore assigned values equal to zero. At the middle of the beam, the longitudinal displacements (u_z) and rotations about the x and y-axes (θ_x and θ_y) are also restrained for all nodes in the section. The loading is applied

to the top surface of the beam in displacement control through two concentrated loads along the full length or one loading point when half the span is considered.

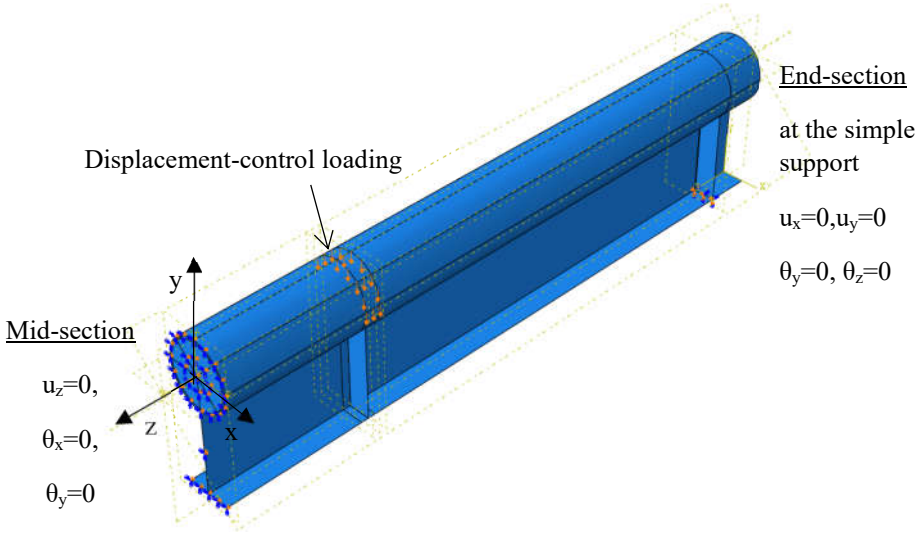

Figure 3: FE model for the CFTFG, including support and loading conditions

2.4 Validation of the load-displacement response

The load-displacement response of the CFTFG from both the FE model and the experimental programme by Wang et al. [12] is presented in Figure 4. Overall, the simulated load-deformation curves are shown to reflect the experimental behaviour very well and the model also provides an excellent prediction of the ultimate load capacity of the CFTFG. The slight variation between the FE and experimental responses presented in the figure could be due to one or a combination of several factors such as the influence of residual stresses which are not included in the FE simulation or the material modelling assumptions.

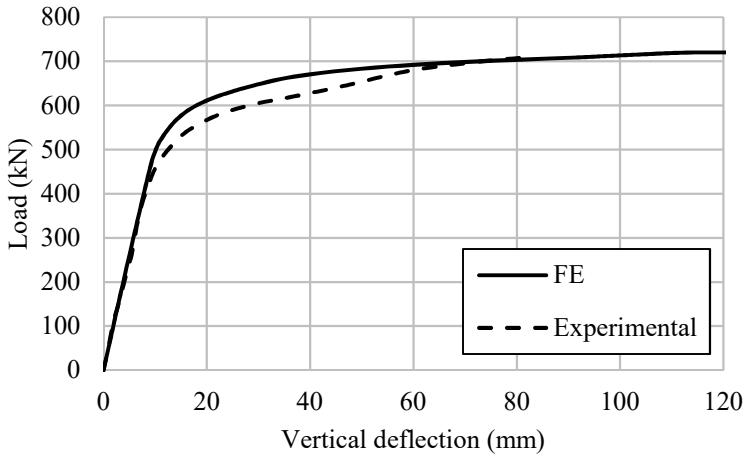

Figure 4: Load versus deflection relationship from the FE analysis and experimental results

3 PARAMETRIC STUDY

The finite element model presented in the previous section was validated against the test conducted by Wang et al. [12] and was shown to provide a reliable and accurate prediction of the response. In the current section, the finite element model is used to study the interaction of sagging bending and axial tension on CFTFGs with various models steel beam sections. In this example, positive (or sagging) bending moment is acting simultaneously with axial forces in the beam. A schematic representation of the static system, loading conditions, and internal force diagrams of the beam under consideration is shown in Figure 5. In order to generalise the results and to specify a reliable moment-axial force (M–N) interaction diagram, a parametric study is conducted using a series of beams with different design parameters. The girders are transversally stiffened at a distance of 1500 mm apart with double-sided flat plate stiffeners with a thickness equal to 12 mm at the support and loading locations. The material properties are similar to those tested experimentally by Wang et al. [12], while the geometries are modified. The thickness of the lower flange (t_f) is taken as the original 14 mm and increased to 28 mm to raise the flexural capacity of the girders, whilst the tube diameter is also varied. The thickness of the tube and web are kept fixed at 8 and 6 mm, respectively. In the generated models, the web slenderness is fixed (h_w) at 267 mm. The geometrical details of the models are given in Table 3.

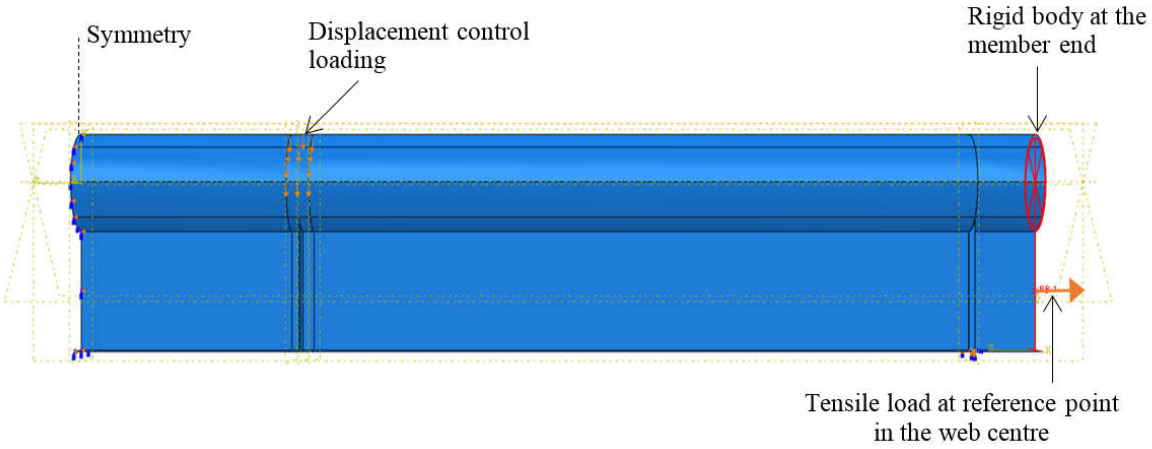

(a) Details of the finite element model

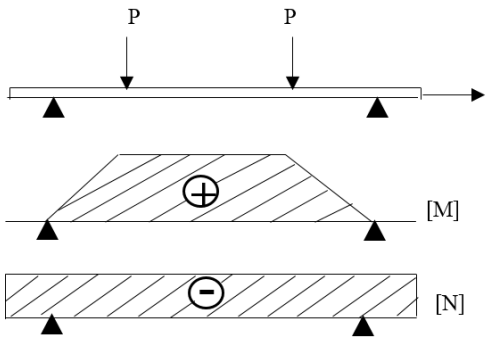

(b) Static system and internal force diagrams

Figure 5: Schematic representation of the structural system considered in the design example

Table 3: Details and FE strengths of CFTFGs.

CFTFGs Group	Specimen	Geometric details				N_u (kN)	M_u (kNm)	PNA location, y_l (mm)
		L (mm)	D_{tube} (mm)	h_w (mm)	t_f (mm)			
G1	GR1	4300	180	267	14	-2310.52	454.3	137.1
	GR2				28	-2915.32	667.2	152.4
G2	GR3		200		14	-2455.21	494.6	146.8
	GR4				28	-3060.01	717.2	160.9
G3	GR5		219		14	-2592.67	544.6	155.9
	GR6				28	-3197.47	760.3	169.2

In this study, an initial geometrical imperfection of L/1000 is derived from an elastic buckling analysis and then introduced into the FE model in the nonlinear load-displacement analysis, where L denotes the span of the girder. For the CFTFGs, buckling takes place in the lateral-torsional mode as the web becomes stiffened transversally at the mid-span location, causing lateral buckling to dominate, rather than the web distortions; Figure 6 shows the buckling mode of the tested girder.

In this paper, it is assumed that the axial force acts on the steel beam only, which is a realistic scenario. The beam is subjected to combined positive bending and axial tension. Constant vertical loads are applied and the distance between the two loading points is 1 m. Various levels of axial tension are studied, ranging from 10% to 80% of the ultimate axial strength of the steel section [1, 14]. For illustration, Figure 7 shows the various responses for the beam GR1. Thus, the axial capacity of a CFTFG can be defined, with reasonable safety, as the axial capacity of the steel section alone, N_u, determined as the sum of the tensile strengths of the loaded steel areas:

$$N_u = A_s f_y \tag{1}$$

where A_s is the area of steel.

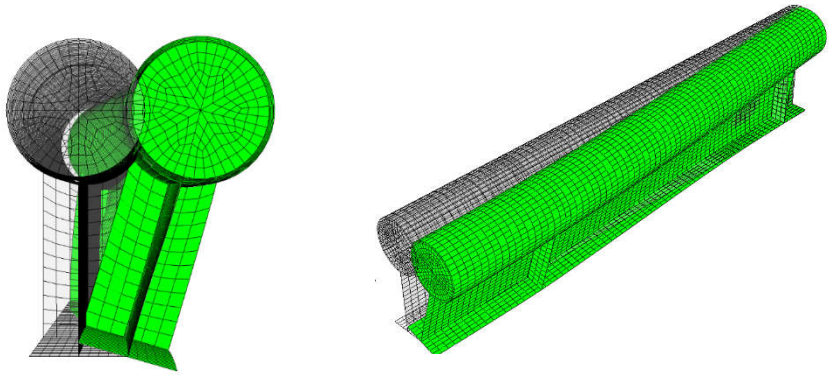

Figure 6: View of the finite element model in both the undeformed and deformed positions

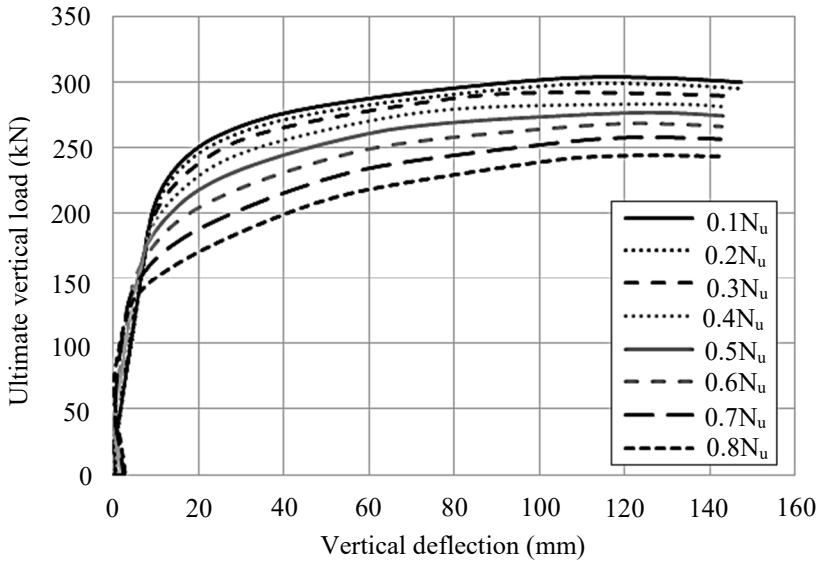

Figure 7: Load–deflection curves of GR1 with various levels of axial tension ranging from 0.1 to 0.8 of the ultimate axial strength of the steel section

4 LOADING AND SOLUTION METHOD

The vertical load is applied as an imposed displacement on the top of the beam, while the axial load is applied as an edge pressure on the steel beam section. The combined loading analysis consists of adding a step in the procedure wherein the axial loads are applied simultaneously to the bending moments. The static nonlinear solution algorithm with adaptive stabilisation as a fraction of dissipated energy is employed to solve for the nonlinear response of the CFTFG. Finite element analysis with concrete elements in tension may result in convergence problems. To avoid these, the discontinuous analysis option is also used in the general solution control options.

Combined axial and vertical loading, large deformations and associated eccentricities make the interpretation of the results cumbersome in the ABAQUS model. To obtain different levels of axial tension, the increments of applied axial load are varied. Afterwards, equilibrium with external loads is checked to ensure accuracy. The moment in each specimen is calculated taking into account the equilibrium of the external forces acting on it. The following equation is used to calculate the ultimate bending moment:

$$M = Pa + Ne \tag{2}$$

where P is the vertical force applied on the beam, a is the distance between the simple support and the vertical force, N is the horizontal force applied placed through a reference point in the steel web, and e is the eccentricity between the location of the axial load and the plastic neutral axis of the CFTFG. The eccentricity is estimated by:

$$e = \left(D_{tube} + \frac{h_w}{2}\right) - y_1 - \delta \tag{3}$$

where y_1 is the depth of the plastic neutral axis (PNA), measured from the top of the section; and δ is the measured vertical deflection at the midspan.

5 INTERACTION DIAGRAM

The positive bending moment versus the corresponding axial tension achieved by all specimens and obtained by the ABAQUS model are plotted in the interaction diagrams for different tube diameters in Figure 8. In general, all CFTFG beams behaved well, exhibiting high ductility levels. In fact, no sudden collapse of any structural component occurred, and failure is gradual during the simulation. The resulting interaction diagrams for beams with h_w = 267 mm are plotted in Figs. 8a and 8b for t_f=14 and 28 mm, respectively. The division into different groups is for ease of visualization. It is evident that the interaction diagrams for all beams follow a comparable trend. A general conclusion is that the moment capacity is reduced with the increase in axial tensile force acting in the steel beam section, as expected. The reduction in moment capacity appears to follow a bilinear trend. At any point along the curve, the moment is almost linearly reduced by the increase in axial load. The developed model is used to conduct further parametric studies on these types of beams and derive more accurate and reliable interaction relationships, as discussed within the following sections.

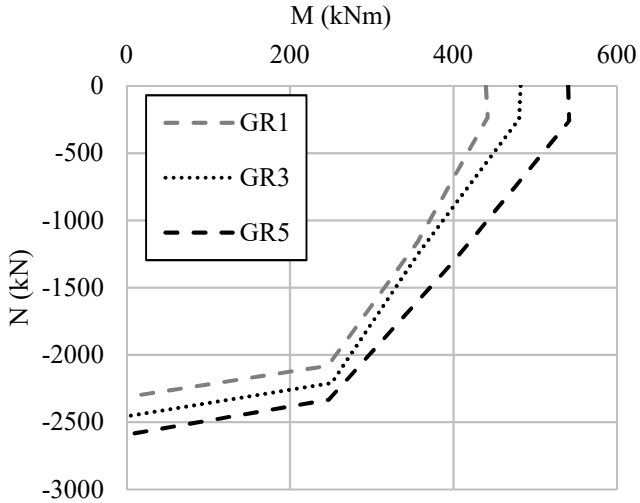

(a)

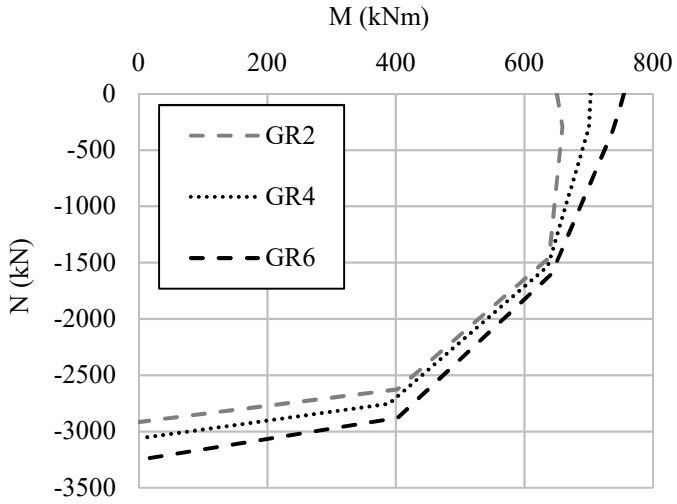

(b)

Figure 8: Moment–axial force interaction diagram for the parametric beams with CFTFGs.

6 ILLUSTRATIVE EXAMPLE

An illustrative example is presented to explain the application of the procedure proposed herein for the prediction of the combined effects of positive bending and axial tension of simply supported CFTFGs. Here, girder GR1 is chosen as an example to show how the combined load of a CFTFG can be estimated, with reference to Table 4. To calculate the combined of positive bending and axial tension of the CFTFG GR1, the following procedures is suggested:

1. Calculate of the ultimate axial load of the girder using Eq. 1.
2. Decide what level of axial tension is acting simultaneously with the bending moment, ranging from 0.1 to 0.8 of the ultimate axial strength of the steel section.
3. Calculate the eccentricity between the location of the axial load and the plastic neutral axis of the CFTFG using Eq. 3.
4. Calculate the moment (kNm) using Eq. 2

Table 4: Details of information solution of GR1.

N/N_u	P_u (kN)	δ (def), mm	e (mm)	N (kN)	M (kNm)
0.1	303.76	116.81	59.58	-231.05	441.88
0.2	298.68	116. 42	59.97	-462.10	420.30
0.3	291.80	104.73	71.67	-693.16	388.03
0.4	283.69	125.99	50.40	-924.21	378.96
0.5	276.82	125.53	50.86	-1155.26	356.48
0.6	268.31	121.94	54.45	-1386.31	326.98
0.7	258.25	126.22	50.17	-1617.36	306.22
0.8	243.93	128.06	48.33	-1848.42	276.56

7 CONCLUSION

A general conclusion is that the moment capacity is reduced with the increase in axial tensile force acting in the steel beam section. The reduction in moment capacity seems to follow a bilinear trend. Any point along the curve in which the moment is almost linearly reduced by the increase in axial load. The following concluding remarks are also presented:

- The numerical simulations demonstrated that it is important to account for the axial force in the design of CFTFGs which are subjected to combined loading.
- Numerical simulations demonstrated that the positive moment capacity of a CFTFG is significantly reduced under the simultaneous action of a relatively high axial tensile force.
- The developed three-dimensional nonlinear finite element model can be used as a tool for the assessment of the nonlinear behaviour and the ultimate failure modes of CFTFGs under combined positive bending and axial tension.

When the beam is subjected to combined tension and flexure, the failure mode depends on the percentage of axial force being applied as the amount of axial load introduced in the steel beam increases, the moment capacity is reduced by increasing the tensile force acting on the steel beam section and a bilinear trend can also be assumed.

REFERENCES

[1] Vasdravellis G., Uy B., Tan E.L. and Kirkland B., "The effects of axial tension on the sagging-moment regions of composite beams", *Journal of Constructional Steel Research*, 72:240-53, 2012.

[2] Wassef W. G., Ritchie P. A. and Kulicki, J. M., "Girders with corrugated webs and tubular flanges—An innovative bridge system" In Proceedings, 14th Annual Meeting, International Bridge Conference, Pittsburgh, Pennsylvania, pp. 425-432. 1997.

[3] Abbas H. H., Sause R. and Driver R. G., "Analysis of flange transverse bending of corrugated web I-girders under in-plane loads", *Journal of Structural Engineering*, 133(3), 347-355, 2007.

[4] Abbas H. H., Sause R. and Driver R. G., "Behavior of corrugated web I-girders under in-plane loads", *Journal of Engineering Mechanics*, 132(8), 806-814, 2006.

[5] Wimer M.R. and Sause R., "Rectangular tubular flange girders with corrugated and flat webs", ATLSS report 04-18. Bethlehem (PA, USA): ATLSS Engineering Research Center, Lehigh University; 2004.

[6] Sause R., Kim B.G. and Wimer M.R., "Experimental study of tubular flange girders", *Journal of structural engineering*, 134(3), pp.384-392, 2008.

[7] Kim B.G. and Sause R., "Lateral torsional buckling strength of tubular flange girders", *Journal of structural engineering*, 134(6), pp.902-910, 2008.

[8] Uy B. and Tuem H.S., "Behaviour and design of composite steel-concrete beams under combined actions", In Proceedings of the 8th International Conference on Steel-Concrete Composite and Hybrid Structures (ASCCS), 2006.

[9] *European Committee for Standardization. Eurocode 4*., design of composite steel and concrete structures. CEN, 1994.

[10] *Standards Australia. Composite structures Part 1:* simply supported beams. AS 2327.1-2004. Sydney (Australia); 2004.

[11] *ANSI/AISC 360-05*., Specification for structural steel buildings. Chicago (IL, USA): American Institute of Steel Construction; 2005.

[12] Wang C. S., Zhai X. L., Duan, L. and Li B. R., "Flexural limit load capacity test and analysis for steel and concrete composite beams with tubular up-flanges", In SHEN Z Y. Proceedings of the 12th Interna-tional Symposium on Tubular Structures. Boca Raton: CRC Press, pp. 413-420, 2008.

[13] Ding Y., Zhang Y. and Zhao J., "Tests of hysteretic behavior for unbonded steel plate brace encased in reinforced concrete panel", *Journal of Constructional Steel Research*, 65(5), pp.1160-1170, 2009.

[14] Vasdravellis G., Uy B., Tan E.L. and Kirkland B., "The effects of axial tension on the hogging-moment regions of composite beams", *Journal of Constructional Steel Research*, 68(1), pp.20-33, 2012.